Paleomagnetism and fission-track ages of Oki-Dogo Island in Southwest Japan

Takeshi Kojima[1], Makoto Okada[1], Hiroto Ohira[2], Katsuyasu Tokieda[2], Hiroaki Komuro[2], and Kazuo Amano[1]

[1]*Department of Environmental Sciences, Ibaraki University, Mito 310-8512, Japan*
[2]*Department of Geoscience, Shimane University, Matsue 610-8504, Japan*

Zircon fission-track (F.T.) ages and paleomagnetic directions were measured on the Neogene series of the Oki-Dogo Island. The results of F.T. dating on the the Tokibariyama Formation show ages of 23.7 ± 1.3 and 20.0 ± 2.3 Ma, indicating the early Early Miocene. Paleomagnetic measurements of the Tokibariyama, Kori Formations (24–17 Ma) and the Oki Trachyte-Rhyolite (6.8 Ma) were done to reveal the movement of Oki-Dogo Island during the Japan Sea opening. The Tokibariyama and Kori Formations show an average declination of $39.9°$. The Oki Trachyte-Rhyolite has the same average geomagnetic direction as the present day value. These results show that a clockwise rotation of $40° \pm 15°$ of the Oki-Dogo Island occurred between 17 and 6.8 Ma which is similar to the main land of southwest Japan.

1. Introduction

The debate on the differences in the paleomagnetic declinations of the Japanese Islands was initiated by Kawai *et al.* (1961). They proposed a Cretaceous-Tertiary tectonic hypothesis that the present bow-shaped Japanese islands were formed by bending. Otofuji *et al.* (1985) reported paleomagnetic data indicating a counterclockwise rotation of $47°$ of northeast Japan and a clockwise rotation of $56°$ of southwest Japan between 21 and 11 Ma. Otofuji *et al.* (1991) concluded 80% of the rotation of southwest Japan occurred at around 15 Ma during a period less than only 2 m.y. On the other hand, deep sea drilling in the Japan Sea provided a result showing that the ocean floor of the Japan Sea formed between 28 and 18 Ma (Tamaki *et al.*, 1992). Jolivet *et al.* (1995) proposed the idea that a part of the $50°$ clockwise rotation of southwest Japan was due to internal deformation of the rotating blocks with second order dominoes. The debate on the timing and the mechanism of the opening of the Japan Sea is still continuing.

The Oki-Dogo Island, where a Neogene series is widely distributed covering the Oki Metamorphic and Granitic Rocks unconformably, is located in the southwestern part of the Japan Sea (Fig. 1). The Tokibariyama, Kori, and Kumi Formations, which were formed during the Japan Sea opening, mainly consist of calc-alkaline volcanic rocks and fluvial-shallow marine deposits (Yamasaki, 1992). The Oki Trachyte-Rhyolite, which was formed after the Japan Sea opening, is distributed in the western part of Oki-Dogo Island. This series is, therefore, a good object to test the model of the Japan Sea opening. Ito (1970) reported paleomagnetic data of the Oki-Dogo Island, however this data is insufficient to discuss the movement of the Oki-Dogo Island because all of the paleomagnetic samples are after Late Miocene. We

carried out paleomagnetic studies and fission-track (F.T.) dating of the series to clarify the timing of the movement of the Oki-Dogo Island related to the Japan Sea opening.

2. Geological Setting

Figures 1 and 2 show the Neogene stratigraphy and the geological map of the study area, respectively. The Neogene series consists of the Tokibariyama, Kori, Kumi, and Tsuma Formations, Oki Trachyte-Rhyolite, and Tsuzurao Quarts Rhyolite, in ascending order. We describe in detail the stratigraphy and the geological structures of the Tokibariyama, Kori, Kumi Formations and the Oki Trachyte-Rhyolite, from which samples were collected for F.T. dating and paleomagnetism.

2.1 Stratigraphy

The Tokibariyama Formation is divided into the lower and upper members according to lithology (Yamasaki, 1992). The lower member is in fault contact with the basememt and partly unconformably overlies the basement. It is mainly composed of rhyolitic pyroclastic rocks and also contains andesite lavas and mudstone. The upper member is mainly composed of andesite lavas and intercalates andesitic pyroclastic rocks, dacite lavas and dacite pyroclastic rocks. The F.T. ages (26.0 ± 4.2 Ma; Kano and Nakano, 1985) of zircon and the K-Ar age (19.7 ± 0.6 Ma; Tainosho *et al.*, 1991) of the potassium feldspar of the younger granite, which intruded into the Tokibariyama Formation (Yamasaki, 1991), show that the Tokibariyama Formation was deposited after the Oligocene (Yamasaki, 1992).

The Kori Formation is divided into the Koji Tuff, Ohzuku Conglomerate, Kori Basalt, Nagu Volcanic, and Togo Basalt Members (Yamasaki, 1991, 1992). This formation unconformably overlies the Tokibariyama Formation. The Kori Basalt, Nagu Volcanic and Togo Basalt Members are contemporaneous heterogeneous facies with the Koji Tuff and the Ohzuku Conglomerate Members (Yamasaki, 1992). The

Age		Ma	Formations and Members	Radiometric ages	Fossils
Pleisto-cene		1	Misaki Basalt / Nijiyama Gravel Beds / Saigo Basalt / Togo Gravel Beds	● 0.82±0.05	
Plio-cene		2 / 3 / 4	Omine Basalt	● 3.3±0.12	
		5	Tsuzurao Qz. Rhyoite	+ 5.0±0.2 (OKI-7)	
Miocene	Late		Hei Trachyte / Oki Trachyte-Rhyolite / Tsuma Formation	■ 6.8±0.2	*Miyagipecten matsumoriensis*
		10	Kumi Formation — Igo Mudstone M. / Iinoyama Diatomite M. / Utagi Mudstone M.		* *D.dimorpha* zone / * *T.yabei* zone / * *D.praedimorpha* zone / * *C.nicobarica* zone
	Middle	15	Kumi Sst. M. / Hei Tuff-Siltstone Alt.M.	○ 14.6±0.7	* *D.hyalina* zone / * *D.lauta* zone / N7-N9, *Miogypsina,Operculina* / Kadonosawa type flora / * *C.kanayae* zone / Daijima type flora
	Early	20	Ko — N O K T / Koji Tuff M.	○ 19.9±1.4 / ○ 21.2±1.0 / ○ 21.3±1.3 / ○ 21.9±1.3	Daijima type flora
			upper m.	+ 20.0±2.3 (OKI-15)	
Oligocene		25	To — lower m.	+ 23.7±1.3 (OKI-13)	

Legend:
(This study) + F.T. age
(Previous studies) ○ F.T. age
■ Rb-Sr age
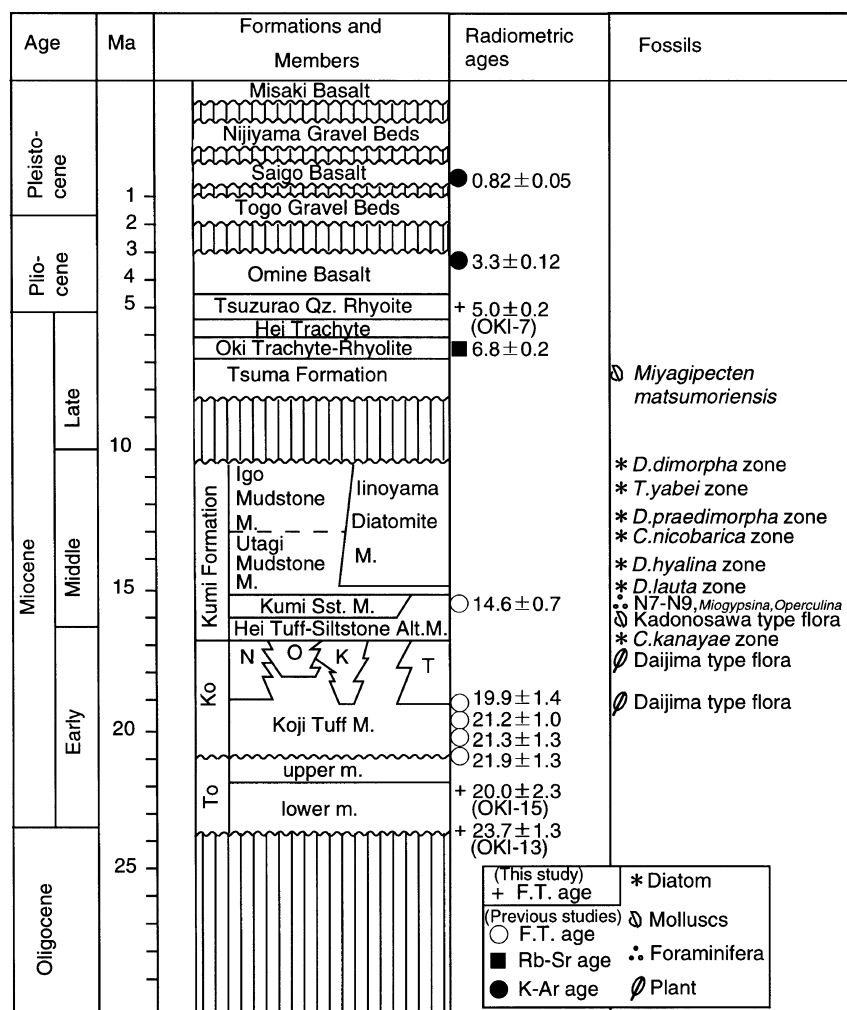● K-Ar age
* Diatom
Molluscs
Foraminifera
Plant

Fig. 1. Schematic columnar section. To: Tokibariyama Formation, Ko: Kori Formation, N: Nagu Volcanics Member, O: Ohzuku Conglomerate Member, K: Kori Basalt Member, T: Togo Basalt Member, Alt.: Alternation, M.: Member, Sst.: Sandstone, Qz.: Quartz. After Iwata *et al.* (1988), Kaneoka *et al.* (1977), Kojima *et al.* (1995), Okubo and Takayasu (1980), Sawada *et al.* (1999), Yamasaki (1992), Yamasaki and Gansawa (1989), and Yokota (1984).

Kori Basalt Member is distributed in the northern part of the Oki-Dogo Island and composed of basalt lavas, basaltic pyroclastic rocks, and volcanic conglomerate. Most of these basalt lavas are auto-brecciated. The Nagu Volcanic Member is distributed on the west coast of the Oki-Dogo Island and composed of basalt lavas, basaltic pyroclastic rocks, volcanic conglomerate and volcanic sandstone. The Togo Basalt Member is distributed on the east coast of the Oki-Dogo Island and composed of auto-brecciated clinopyroxene-olivine basalt lavas. The zircon F.T. ages of the Koji Tuff Member were reported as 21.2 ± 1.0 Ma by Yamasaki and Ganzawa (1989) and as 19.9 ± 1.4, 21.3 ± 1.3, 21.9 ± 1.3 Ma by Yoshitani *et al.* (1995). Geological age of the Kori Formation is thought to range from the early Middle Miocene to the early Late Miocene based on the Daijima type flora and the F.T. ages of the Koji Tuff Member and F.T. age (14.6 ± 0.7 Ma; Yamasaki and Ganzawa, 1989) of the Kumi Formation.

The Kumi Formation is divided into five members of the Hei Tuff and Siltstone Alternation, Kumi Sandstone, Utagi Mudstone, Igo Mudstone, and Iinoyama Diatomite Members (Yamasaki, 1991). This formation conformably over-lies the Kori Formation. The Hei Tuff and Siltstone Alternation Member is composed of fine-coarse grained acidic tuff, pumice tuff, and siltstone alternation. The Kumi Sandstone Member is contemporaneous heterotopic facies with the Hei Tuff and Siltstone Alternation Member, and is composed of medium sandstone and mudstone alternation, pebble-granule conglomerate and acidic tuff. The lower part of the Iinoyama Diatomite Member is made of massive diatomite and interfingered with the Utagi Mudstone Member which is composed of black-gray mudstone and fine-coarse sandstone, whereas, the upper part of the Iinoyama Diatomite Member is also interfingered with the Igo Mudstone Member which is composed of massive sandy mudstone and fine-coarse sandstone (Yamasaki, 1992). Most of the Utagi Member is distributed in the southern part of the Oki-Dogo Island, and conformably overlies the Hei Tuff and Siltstone Alternation and the Kumi Sandstone Members. Geological age of the Kumi Formation is thought to be the early Late Miocene–the middle Late Miocene based on the foraminiferal assemblage (Okubo and Takayasu, 1980), the diatom assemblage (Yokota, 1984; Yamasaki *et al.*, 1990; Yamasaki, 1992) and on F.T. ages
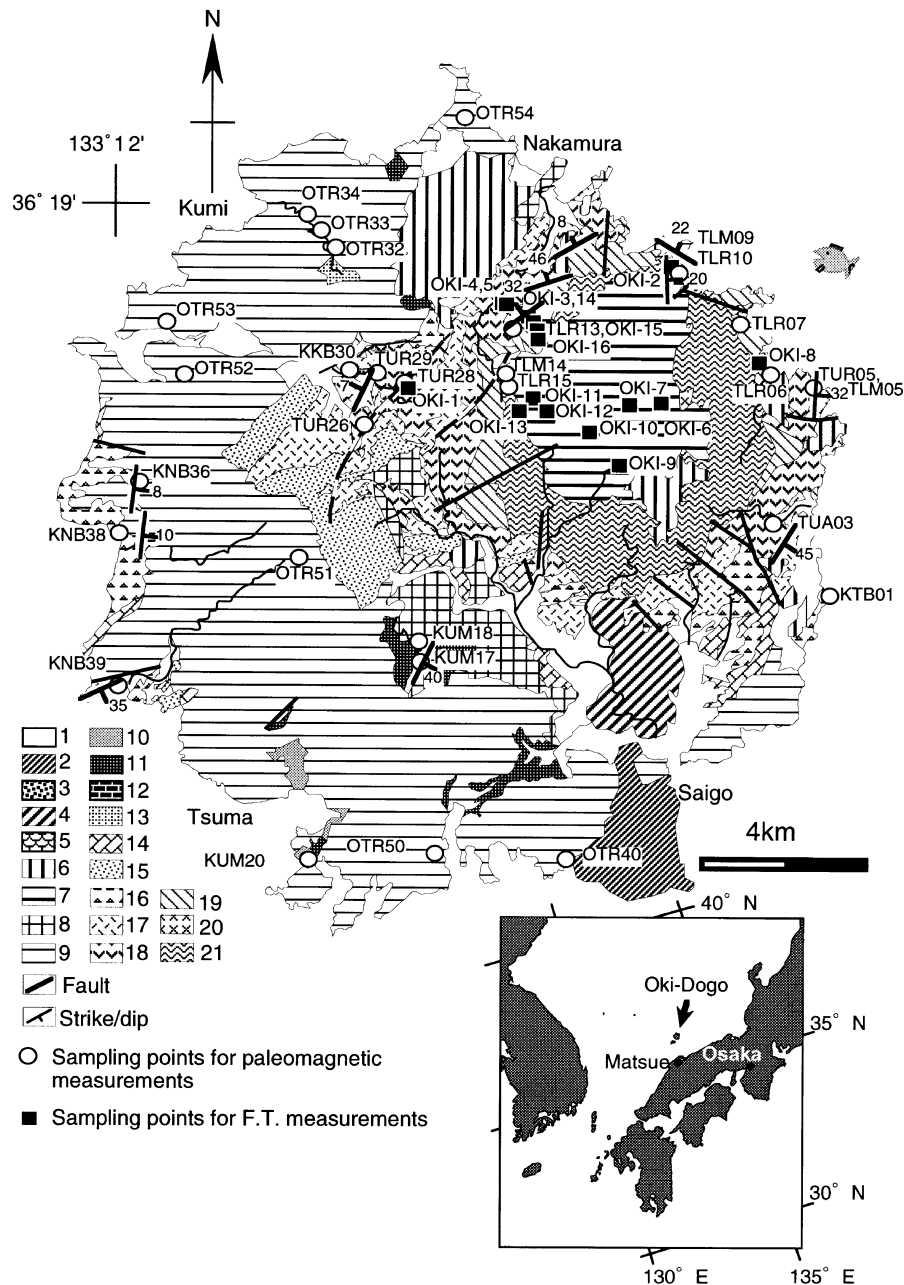
Fig. 2. Locality map of the Oki-Dogo Island and geological map. 1: Alluvium, 2: Misaki Basalt, 3: Nijiyama Gravel Beds, 4: Saigo Basalt, 5: Togo Gravel Beds, 6: Omine Basalt, 7: Tsuzurao Quartz Rhyolite, 8: Hei Trachyte, 9: Oki Trachyte-Rhyolite, 10: Tsuma Formation, 11~14: Kumi Formation (11: Igo Mudstone Member/Utagi Mudstone Member, 12: Iinoyama Diatomite Member, 13: Kumi Sandstone Member, 14: Hei Tuff-Siltstone Alternation Member), 15~17: Kori Formation (15: Ohzuku Conglomerate Member, 16: Togo Basalt, Kori Basalt, and Nagu Volcanics Members, 17: Koji Tuff Member), 18~19: Tokibariyama Formation (18: upper member, 19: lower member), 20: Younger granite, 21: Basement Rocks (Oki Metamorphics and Granite). After Kojima et al. (1995), Sawada et al. (1999), and Yamasaki (1992).

(14.6 ± 0.7 Ma: Yamasaki and Ganzawa, 1989).

The Oki Trachyte-Rhyolite is widely distributed in the western part of the Oki-Dogo Island. It is composed of rhyolite and trachyte lavas and pyroclastic rocks, and unconformably overlies the Tokibari, Kori, Kumi, and Tsuma Formations. This formation was not tectonically deformed. Iwata et al. (1988) reported the Rb-Sr whole-rock isochron age of 6.8 ± 0.2 Ma.

2.2 Geological structures

The study area is characterized by a dome structure in the Tokibariyama and Kori Formations. The basement rocks, which are covered by the Tsuzurao Quartz Rhyolite unconformably, crop out in the core of the dome. The north-western part of the dome dips gently to the northwest, whereas the eastern part dips steeply to the east. In the western half of the study area, a syncline with an axis trending N-S exists in the Kori and Kumi Formations, and the Oki Trachyte-Rhyolite is horizontally distributed covering this syncline unconformably.

3. Fission-Track Dating
3.1 Samples and measurements

We collected samples from 15 sites for F.T. dating shown in Fig. 2 and Table 1, and obtained reliable data from 3 samples of OKI-7, 13, and 15. OKI-7 is from rhyolitic auto-brecciated lava of the Tsuzurao Quartz Rhyolite. OKI-13 and OKI-15 are the matrix of rhyolitic lapilli tuff and rhyolitic coarse tuff of the lower member of the Tokibariyama Formation.

All the samples were crushed to 75–250 μm fraction. After panning, heavy liquid separation and magnetic separation, zircon grains were picked out by hand. Zircon grains were immersed in 45% HF at 80°C for 2 hours to remove minute glasses, rock fragments and minerals clinging to the grains. After this treatment, 300 grains of zircon were taken from 3.3 kg of OKI-7, 300 grains from 5.0 kg of OKI-13 and 200 grains from 5.0 kg of OKI-15.

The age determination was done by the external detector method with zeta calibration (Hurford, 1990). The zircon grains were mounted in PFA Teflon sheets. Crystal external (2π) surfaces were used for OKI-13 and OKI-15, however crystal internal (4π) surfaces were used for OKI-7 because its crystal external (2π) surfaces had many scars. Etching was done using KOH-NaOH melt at 225°C. OKI-7, OKI-13, and OKI-15 were etched for 77, 76, and 49 hours, respectively. The zircon mounts and a standard glass (NIST, SRM-612) were covered by uranium-free muscovite detectors and were irradiated with thermal neutron in a pneumatic tube (cd-ratio: 3.5) of JRR-4 of Japan Atomic Energy Research Institute (Tokai village). After the irradiation, muscovite detectors were eched in 48% HF for 30 minutes at room temperature. We used zeta values of 343.6 (for the 2π surface), and 350.6 (for the 4π surface) determined for dosimeter glass SRM-612 using the Fish Canyon Tuff and Buluk Member Tuff (Hurford, 1990).

3.2 Results of F.T. dating

The results of the measurements are shown in Table 2. These passed χ^2-test by over 5%.

The age of OKI-13 and OKI-15 are 23.7 ± 1.3 and 20.0 ± 2.3 Ma, respectively. These ages are consistent with the K-Ar age (19.7 ± 0.6 Ma) of the potassium feldspar of the younger granite intruded into the Tokibariyama Formation (Tainosho *et al.*, 1991). These results suggest that the Tokibariyama Formation was formed in the early Early Miocene.

The age of OKI-7 is 5.0 ± 0.2 Ma. The sample of OKI-7 was considered to belong to the Tokibariyama Formation according to a previous study (Yamasaki, 1992), however we suggest the possibility that OKI-7 pertains to the Tsuzurao Quartz Rhyolite based on its age.

4. Paleomagnetism
4.1 Samples and measurements

We collected paleomagnetic samples from a total of 30 sites at 4 stratigraphic units (Oki Trachyte-Rhyolite, Kumi, Kori, and Tokibariyama Formations) consisting of the Miocene volcanic sedimentary strata in Oki-Dogo Island (Fig. 2, Table 1). More than five cores drilled by a standard size portable engine corer or three hand-picked samples were taken from each site. All the samples were oriented by a magnetic compass. In the laboratory, three or more cores were drilled from each hand-picked sample, and cut into two

Table 1. Fission-track and Paleomagnetic samples of Oki-Dogo Island.

F.T. samples

site	Latitude N	Longitude E	Rock type
OKI-1	36°16.5′	133°16.0′	Rhyolite lava
OKI-2	36°18.5′	133°19.7′	Rhyolite lava
OKI-3	36°17.5′	133°17.6′	Rhyolite tuff
OKI-4	36°17.6′	133°17.4′	Dacite lava
OKI-5	36°17.6′	133°17.5′	Andesite lava
OKI-6	36°16.3′	133°20.2′	Andesite lava
OKI-7	36°16.2′	133°19.9′	Rhyolite lava
OKI-8	36°16.6′	133°21.8′	Rhyolite tuff
OKI-9	36°15.3′	133°19.7′	Rhyolite tuff
OKI-10	36°16.0′	133°19.2′	Rhyolite tuff
OKI-11	36°16.2′	133°18.3′	Rhyolite tuff
OKI-12	36°16.2′	133°18.0′	Rhyolite tuff
OKI-13	36°16.0′	133°17.6′	Rhyolite tuff
OKI-14	36°17.5′	133°17.6′	Rhyolite tuff
OKI-15	36°17.4′	133°17.8′	Rhyolite tuff
OKI-16	36°17.3′	133°17.8′	Rhyolite tuff

Paleomagnetic samples
N: number of rock samples

site	N	Latitude N	Longitude E	Rock type
Oki Trachyte-Rhyolite				
OTR32	4	36°18.3′	133°15.0′	Rhyolite lava
OTR33	4	36°18.5′	133°14.8′	Rhyolite lava
OTR34	3	36°18.7′	133°14.7′	Rhyolite lava
OTR40	5	36°10.8′	133°18.8′	Rhyolite lava
OTR50	7	36°10.5′	133°16.7′	Rhyolite lava
OTR51	3	36°14.3′	133°14.7′	Rhyolite lava
OTR52	4	36°14.7′	133°12.8′	Rhyolite lava
OTR53	7	36°17.3′	133°12.5′	Rhyolite lava
OTR54	6	36°20.2′	133°17.2′	Rhyolite lava
Kumi Formation				
KUM17	3	36°12.8′	133°16.1′	Mudstone
KUM18	5	36°13.2′	133°16.0′	Mudstone
KUM20	7	36°10.3′	133°14.8′	Mudstone
Kori Formation				
KTB1	3	36°13.7′	133°22.8′	Basalt lava
KKB30	9	36°16.8′	133°15.3′	Basalt lava
KNB36	5	36°15.3′	133°12.0′	Basalt lava
KNB38	7	36°15.8′	133°11.5′	Basalt lava
KNB39	5	36°12.8′	133°11.8′	Basalt lava
Tokibariyama Formation				
TUA03	8	36°14.7′	133°22.0′	Andesite lava
TUR05	3	36°16.3′	133°22.5′	Rhyolitic tuff
TLM05	7	36°16.3′	133°22.5′	Mudstone
TUA26	7	36°16.2′	133°15.4′	Andesite lava
TUA28	11	36°16.5′	133°16.0′	Andesite lava
TUA29	5	36°16.7′	133°15.5′	Andesite lava
TLR06	3	36°16.4′	133°21.9′	Rhyolitic tuff
TLR07	7	36°17.2′	133°21.5′	Rhyolitic tuff
TLM09	6	36°18.0′	133°20.6′	Mudstone
TLR10	14	36°17.8′	133°20.5′	Rhyolitic tuff
TLR13	12	36°17.4′	133°17.8′	Rhyolitic tuff
TLM14	6	36°16.9′	133°17.3′	Mudstone
TLR15	6	36°16.8′	133°17.3′	Rhyolitic tuff

Table 2. Fission-track data of zircons from the Tokibariyama Formation and the Tsuzurao Quartz Rhyolite, the Oki-Dogo Island. $\rho(N)$: fission-track density (total number of tracks counted), subscripts s and i for spontaneous and induced tracks in zircons, respectively, and d for induced tracks from the dosimetory glass. OKI-13 and 15 were measured on 2π surface, and OKI-7 was measured on 4π surface using 0.5 for the $4\pi/2\pi$ geometry correction factor. $P(\chi^2)$ is probability of obtaining χ^2 value for v degrees of freedom (where v = No. crystals-1); $P(\chi^2) > 5\%$ is shown. Thermal neutron irradiation was done at pneumatic tube of JRR-4 of Japan Atomic Energy Research Institute (Tokai village). The errors are shown by 1 sigma.

Sample code	No. of crystals	Spontaneous ρ_s (ΣNs) (10^5 $^{-2}$)	Induced ρ_i (ΣNi) (10^5 $^{-2}$)	Dosimeter ρ_d ($\Sigma N\phi$) (10^5 $^{-3}$)	$P(\chi^2)$ (%)	U-content (ppm)	Age ($\pm 1\sigma$) (Ma)	Latitude N	Longitude E
OKI-7	24	1.413 (526)	4.700 (2100)	1.098 (3917)	73.5	640.3	5.0 ± 0.2	36°16.2′	133°19.9′
OKI-13	38	1.133 (739)	1.337 (872)	0.802 (2650)	9.4	602.6	23.7 ± 1.3	36°16.0′	133°17.6′
OKI-15	13	0.695 (180)	1.378 (357)	1.095 (3907)	12.3	461.8	20.0 ± 2.3	36°17.4′	133°17.8′

Table 3. Summary of paleomagnetic results of the Oki-Dogo Island.

N: number of rock samples, D: declination, I: inclination,
k: Fisherian precision parameter, α_{95}: 95% confidence limit

site	N	D deg.	I deg.	k	α_{95} deg.
Oki Trachyte-Rhyolite					
OTR32	4	127.6	−25.9	52.1	12.9
OTR34	3	202.0	−55.1	94.0	12.8
OTR40	5	164.6	−46.0	106.2	7.5
OTR50	7	184.5	−47.3	30.9	11.0
OTR51	3	152.3	−39.6	80.0	13.9
OTR52	4	186.0	−19.1	42.6	14.2
OTR53	7	116.5	−79.9	40.2	9.6
OTR54	6	164.3	−54.1	33.8	11.7

site	N	strike/dip	in-situ D deg.	I deg.	tilt-corrected D deg.	I deg.	k	α_{95} deg.
Kori Formation								
KTB1	3		72.8	29.5			1822.3	2.9
KKB30	9	210/10	225.8	−56.6	225.8	−58.0	26.5	10.2
KNB36	5	18/8	63.9	36.1	67.5	30.2	605.6	3.1
KNB38	7	11/10	25.2	51.6	36.4	48.2	94.9	6.2
KNB39	5	70/35	9.8	28.2	30.1	55.7	374.3	4.0
Tokibariyama Formation								
TUA03	8	45/45	−11.3	38.7	42.8	64.3	15.2	14.7
TUR05	3	12/32	192.2	−60.6	235.3	−47.6	916.1	4.0
TUA26	7	220/7	69.2	61.2	56.8	64.0	66.8	7.4
TUA28	11	220/7	15.4	61.1	5.1	57.6	8.4	16.8
TUA29	5	220/7	72.7	59.2	60.4	62.3	52.3	10.7
TLR10	14	5/20	132.1	−20.8	139.2	−36.1	32.7	7.1
TLR13	12	240/32	212.4	−60.1	184.0	−37.8	33.0	7.7

or more specimens.

Magnetic measurements were performed at Ibaraki University using a cryogenic magnetometer (2G model 750R), alternating field (AF) and thermal demagnetizers (Natsuhara Giken models DEM-8061 and TDE-91E), a low-field susceptibility meter (Bartington MS2) and a pulse magnetizer (Magnetic Measurement MMP9). Magnetic field intensity was less than 5 nT in the thermal demagnetizer sample region.
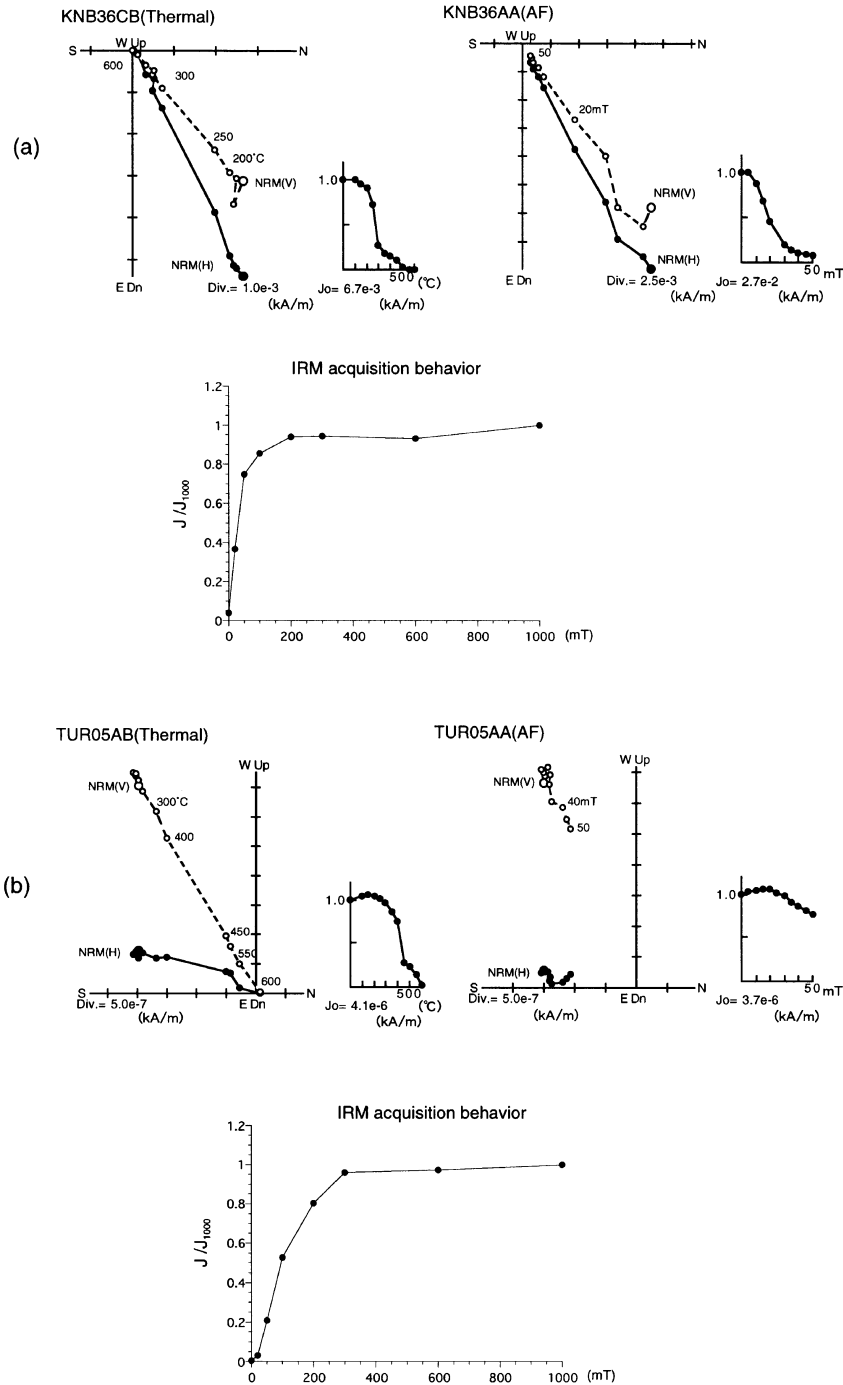
Fig. 3. Orthogonal projections of typical demagnetization behaviors, typical IRM acquisition curves and magnetic susceptibility fluctuations through the thermal runs. In the orthogonal projections, open circle denotes a projection on the N-S vertical plane and closed circle on the horizontal plane. (a) The AF result exhibits similar demagnetization paths with the thermal one at portions higher than 10 mT. (b) and (c) The AF result exhibit different demagnetization paths with the thermal one. IRM acquisition carried out at 20, 50, 100, 200, 300, 600, and 1000 mT, respectively. (d) An example for specimens being not able to yeild ChRMs. (e) Magnetic susceptibility fluctuations through the thermal runs of specimens shown above.

To determine an appropriate demagnetization procedure at each site, we selected two pilot specimens from each site and demagnetized progressively, one thermally and another by AF. The AF demagnetization was statistically done at three orthogonal axes up to 50 mT at 5 mT intervals, and the thermal one from 100°C to 600°C at 50°C intervals. Magnetic susceptibility was measured at each thermal demagnetization step to monitor possible chemical changes caused by

heating. Acquisition of isothermal remanent magnetization (IRM) was progressively performed every 25~50 mT up to 1000 mT to know a specimen's coercivity spectrum.

4.2 Rock magnetic and paleomagnetic results

Stepwise demagnetizations for the pilot specimens yielded characteristic remanent magnetization (ChRM) components at 20 sites (Table 3 and Figs. 3(a), (b), (c) for examples), showing an identical demagnetization pattern in both proce-
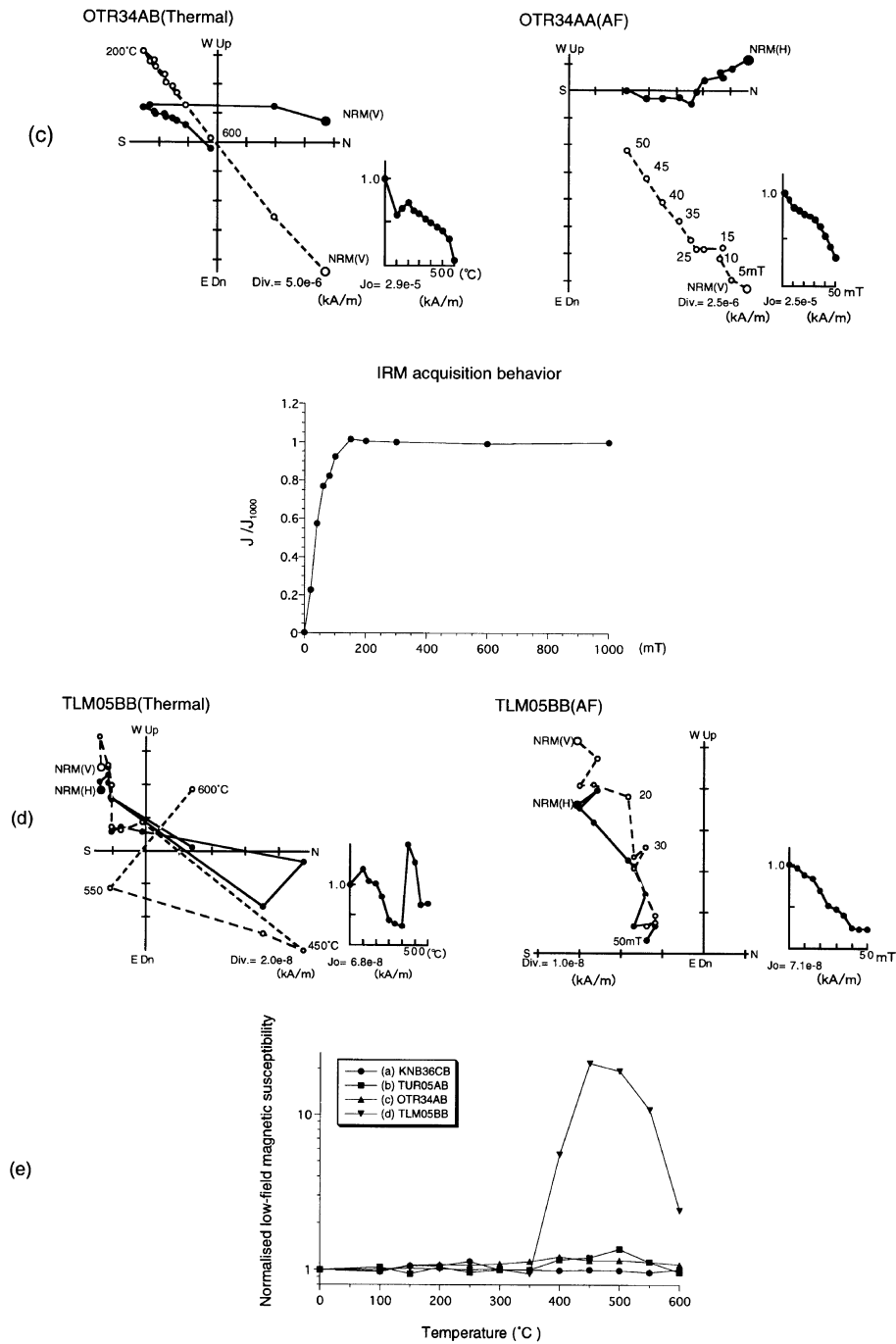
Fig. 3. (continued).

dures at each site. A ChRM was determined by the principal component analysis (Kirschvink, 1980) applied to data composing a liner segment toward the origin on a demagnetization diagram. At other sites, thermal demagnetization exhibits scattered directions above 400°C at which magnetic susceptibility largely goes up, and AF shows that the remanence has not moved to the origin (Figs. 3(d), (e) for examples).

The IRM acquisition was carried out on specimens from the 20 sites where ChRM were extracted. The results exhibit dominant low coercivity of less than 200~300 mT and negligible higher coercivity spectra at the 20 sites (Fig. 3),

indicating low coercivity magnetic minerals like magnetites, maghemites, and magnetic iron sulfides as possible magnetic carriers.

Thermal demagnetization results from the sites producing ChRMs except TUR05 and OTR34 show that the remanence vectors sharply decline from 200° to 300°C, slowly move toward the origin from 300° to 550°C and disappear by 600°C (Fig. 3(a)). This result also shows that the magnetization above 200°C consists of a single component appearing to be a ChRM. The component can be separated into two temperature ranges at around 300°C: i) a dominant lower temperature component, and ii) a minor higher temperature component.
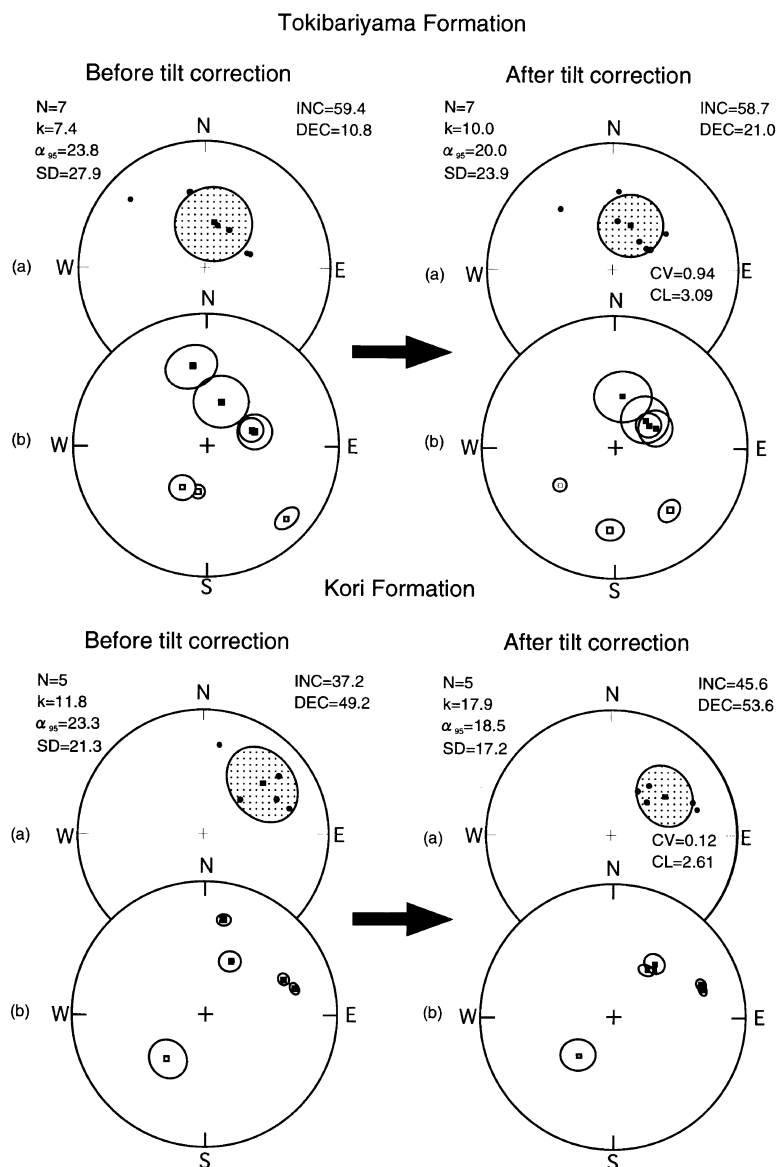
Fig. 4. Comparison of ChRM with before and after tilt correction. (a) Average paleomagnetic directions of the Tokibariyama and Kori Formations with 95% confidence circles. A circle denotes site-mean direction, which is showed by converting reversed directions to normal. Squares and shaded ovals indicate overall means and their 95% confidence limit. *N*: number of sites, *k*: Fisherian precision parameter, α_{95}: 95% confidence limit, SD: standard deviation, Inc: inclination, Dec: declination, CV: correlation value, CL: 95% confidence limit of the correlation valve. CV and CL are used in the correlation test (McFadden, 1990) (b) Equal-area projections of site-mean directions with 95% confidence circles. Solid squares refer to lower hemisphere, and the open squares refer to upper hemisphere.

Since the susceptibility does not change much through the thermal demagnetization runs (Fig. 3(e)), the lower temperature component seems not to be carried by iron sulfides, but by low coercivity magnetites and/or maghemites. The AF results exhibit similar demagnetization paths with the thermal paths at portions higher than 10 mT, suggesting that the ChRMs can be extracted effectively by AF demagnetization. At these sites, therefore, we demagnetized other specimens by AF and extracted components higher than 10 mT as ChRMs.

The result of TUR05 thermal demagnetization shows that the remanent vector declines abruptly between 400 and 450°C, moves straight to the origin and disappears by 600°C. The IRM acquisition curve from this site exhibits saturation at 300 mT. These results indicate that the component higher than the 450°C might be carried by fine grain magnetites having a hard coercivity of close to 300 mT. Since this component is quite stable and is not removed effectively by AF (Fig. 3(b)), we demagnetized other specimens thermally and extracted components of higher than 450°C as ChRMs.

The result of OTR34 thermal demagnetization shows that the remanent vector turns from normal to reversed at 200°C, and it declines toward the origin and disappears by 600°C (Fig. 3(c)). Magnetization higher than the 200°C portion consists of a single component seeming to be a ChRM, and the IRM acquisition curve of this sample shows its saturation by 100 mT indicating that low coercivity minerals dominate the magnetic carriers. These results suggests magnetites as a

magnetic carrier for the ChRM. However, the lower temperature portion which might be a recent overprint is not removed by AF. Thus, we demagnetized other specimens thermally and extracted components higher then $200°C$ as ChRMs.

According to sedimentary structures found near the sampling sites, we performed tilting correction of in-situ paleomagnetic results from all the sites except OTR series (Oki Trachyte-Rhyolite) and KTB1 (Kori Formation) which are thought not to have moved tectonically (Fig. 4). The result of the correction, shown separately for the Tokibariyama and Kori Formations (except KTB1), indicates that the confidential circles are reduced after the correction in both cases (Fig. 4) suggesting that the correction is efficient to provide a better estimation of the remanent directions. To assess whether the correction is significant, we apply the correlation test proposed by Mcfadden (1990). The test takes correlation between the corrected direction and the bedding orientation at each site, sums up all the sites, and compares the sumed correlation value to the confidence limit provided at every number of samples. As the result, the correlation values from both the formations are smaller than the limits (Fig. 4) suggesting the correction is significantly effective.

Fig. 5. Average paleomagnetic directions of before and after of rotation with 95% confidence circles. Circle denotes site-mean direction, which is showed by converting reversed directions to normal. That of the Tokibariyama and Kori Formations is before rotation and that of the Oki Trachyte-Rhyolite is after rotation. Squares and shaded ovals indicate overall means and their 95% confidence limit. N: number of sites, k: Fisherian precision parameter, α_{95}: 95% confidence limit, SD: standard deviation, Inc: inclination, Dec: declination.

Therefore, we use the corrected directions for further discussion.

Since distributions of site mean directions from the Tokibariyama and Kori Formations are similar, we treated these data together as there is no significant tectonic movement between these formations. On the other hand, the distribution of site mean directions from the Oki Trachyte-Rhyolite looks discrepant with those of other formations. The average direction from the Tokibariyama and Kori Formations points significantly in an eastward declination $(40 \pm 15°)$ but the one from the Oki Trachyte-Rhyolite does not show a significant difference from the present axial dipole field direction (Fig. 5). This result suggests that a clockwise rotation of $\sim 40°$ occurred between the age of deposition of the Tokibariyama and Kori Formations and that of the Oki Trachyte-Rhyolite (Fig. 5).

5. Discussion

5.1 Timing of clockwise rotation

The geological age of the Tokibariyama and Kori Formations was determined as the Early Miocene (24–17 Ma) based on the F.T. ages and the Daijima type flora. The Rb-Sr age of the Oki Trachyte-Rhyolite was reported as 6.8 Ma by Iwata *et al.* (1988). The timing of clockwise rotation is between 17 and 6.8 Ma. This result is consistent with that of Otofuji *et al.* (1991).

5.2 Amount of clockwise rotation

The mean paleomagnetic direction of the Tokibariyama and Kori Formations is $D = 39.9°$, $I = 51.8°$, $\alpha_{95} = 15.5°$, and that of the Oki Trachyte-Rhyolite is $D = -14.4°$, $I = 48.5°$, $\alpha_{95} = 18.3°$. The inclination of the Tokibariyama and Kori Formations is not different from that of the Oki Trachyte-Rhyolite, however the declination is different between them. Since the α_{95} area of the Oki Trachyte-Rhyolite contains the geocentric axial dipole field direction of this region, it can be said that the Oki Trachyte-Rhyolite has not been moved tectonically since the deposition. These results indicate that a clockwise rotation of $40° \pm 15°$ occured during the period after the deposition of the Tokibariyama and Kori Formations and before the time of the formation of the Oki Trachyte-Rhyolite.

5.3 Geological evidence for the Japan Sea opening

Transgression started slowly from the early Early Miocene because the Tokibariyama Formation contains lacustrine mudstone beds (Kojima *et al.*, 1995) and the Kori Formation consists of basaltic submarine auto-brecciated lavas and conglomerate. Yamasaki (1992) reported that the Kori Formation and the lower Kumi Formation was deposited in fluvial to shallow sea environments. The timing of the clockwise rotation of the Oki-Dogo Island is consistent with that of the environment change from fluvial-shallow sea to deep sea.

According to the topography and geological structure of the sea floor between Oki-Dogo and the Shimane Peninsula, it is continuous and shows no differential movement. The topography which is shown in Fig. 6 is characterized by smooth continental shelf shallower than 100 m and no large faults were reported (Iwabuchi, 1968). Otofuji *et al.* (1991) reported paleomagnetic data indicating a clockwise rotation of the Kawai Formation, which is correlated with the Kumi Formation in Oki-Dogo based on the geological
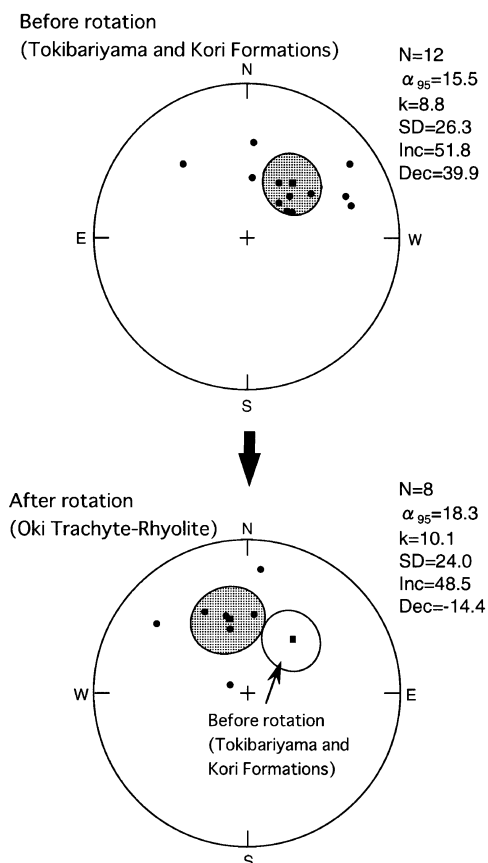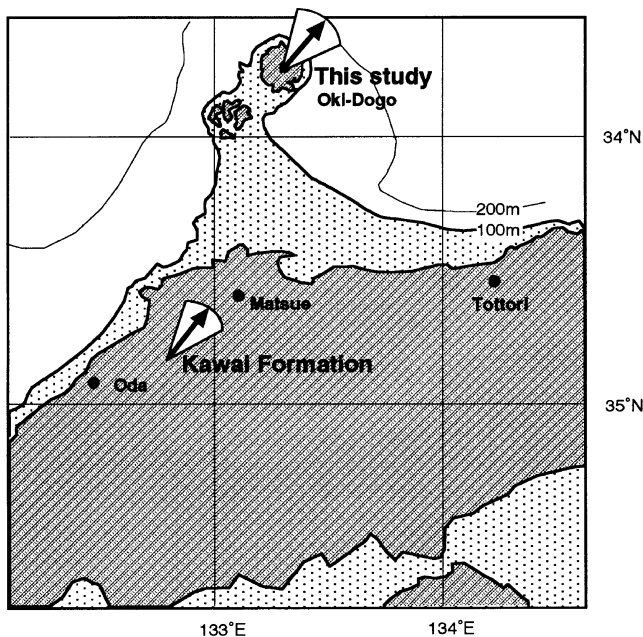
Fig. 6. Bathimetric map and Paleomagnetic declinations in the Chugoku district. The map was made being modified after Igi and Hattori (1991). The mean declinations indicated by the arrows are shown together with their 95% confidence limits ($= \sin^{-1} [\sin \alpha_{95} / \cos I]$, where α_{95} is the radius of the 95% confidence limit and I is the inclination). The declination in the main land of southwest Japan is after Otofuji *et al.* (1991).

age, in the eastern part of Shimane Prefecture. The Kawai Formation consists mainly of sandstone. However, it is comformably covered by or party interfingered with the Kuri Formation composed of black shale and rhyolite-dacite pyroclastic rocks. These facies resemble that of the Kumi Formation (Yamauchi and Yoshitani, 1981). These results show that Oki-Dogo probably rotated together with Southwest Japan.

6.   Conclusions

1.   Paleomagnetic and F.T. age measurements show a clockwise rotation of $40° \pm 15°$ of the Oki-Dogo Island between 17 and 6.8 Ma. This result is consistent with the results of previous studies (e.g. Otofuji *et al.*, 1991).

2.   The timing of the clockwise rotation of Oki-Dogo Island related to the Japan Sea opening almost coincided with the timing of the environmental change from fluvial-shallow sea to deep sea.

References

Hurford, A. J., Standardization of fission track dating calibration: Recommendation by Fission Track Working Group of the I.U.G.S. Subcommision on Geochronology, *Chem. Geol.*, **80**, 171–178, 1990.

Igi, S. and H. Hattori, Geologic Atlas of Japan; Chugoku and Shikoku regions, Under the Supervision of the Geological Survey of Japan, ASAKURA Publishing Company, LTD., Tokyo, 1991 (in Japanese).

Ito, H., Polarity transitions of the geomagnetic field deduced from the natural remanent magnetization of Tertiary and Quaternary rocks in Southwest Japan, *J. Geomag. Geoelectr.*, **22**(3), 273–290, 1970.

Iwabuchi, Y., Submarine Geology of the Southeastern part of the Japan Sea, *Contributions from the Ins. Geo. Paleontology. Tohoku Univ.*, **66**, 1–76, 1968 (in Japanese).

Iwata, M., H. Kagami, E. Takahashi, and H. Kurasawa, The Rb-Sr whole rock isochron age and genesis of Oki Trachyte-Rhyolite Group in Oki Dogo Island, *Bull. Vol. Soc. Japan*, **33**, 79–86, 1988 (in Japanese with English abstract).

Jolivet, L., H. Shibuya, and M. Fournier, Paleomagnetic rotations and the Japan Sea opening, in *Active Margins and Marginal Basins of the Western Pacific*, pp. 355–369, Am. Geophys. Union, Washington, D.C., 1995.

Kano, K. and S. Nakano, Stratigraphic correlation of the Neogene in the San-in district, Southwest Japan, in the light of radiometric dating, *Bull. Geol. Surv. Japan*, **36**, 427–438, 1985 (in Japanese with English abstract).

Kaneoka, I., E. Takahashi, and S. Zashu, K-Ar ages of alkali basalts from the Oki-Dogo Island, *J. Geol. Soc. Japan*, **83**, 187–189, 1977.

Kawai, N., H. Ito, and S. Kume, Deformation of the Japanese Islands as inferred from rock magnetism, *Geophys. J. Roy. astr. Soc.*, **6**, 124–129, 1961.

Kirschvink, J. L., The least-squares line and plane and the analysis of paleomagnetic data, *Geophys. J. Roy. astr. Soc.*, **62**, 699–719, 1980.

Kojima, T., H. Komuro, and H. Murakami, The Tokibariyama Formation in the northeastern part of the Oki-Dogo Island, *Geol. Rept. Shimane Univ.*, **14**, 89–100, 1995 (in Japanese with English abstract).

McFadden, P. L., A new fold test for paleomagnetic studies, *Geophys. J. Int.*, **103**, 163–169, 1990.

Okubo, M. and K. Takayasu, First discovery of Miogypsina in OKI Island, west Japan, *J. Geol. Soc. Japan*, **86**, 37–39, 1980 (in Japanese).

Otofuji, Y., T. Matsuda, and S. Nohda, Opening mode of the Japan Sea inferred from the paleomagnetism of the Japan arc, *Nature*, **317**, 603–604, 1985.

Otofuji, Y., T. Itaya, and T. Matsuda, Rapid rotation of southwest Japan-paleomagnetism and K-Ar ages of Miocene volcanic rocks of southwest Japan, *Geophys. J. Int.*, 1991 (in Japanese with English Abstract).

Sawada, S., A. Toume, S. Kobayashi, H. Komuro, H. Kitagawa, and H. Murakami, Volcanic vent and feeder dikes from the Latest Miocene Tsuzurao Volcanic Rocks, Oki-Dogo, *J. Geol. Soc. Japan*, **105**(4), pictorials, 1999 (in Japanese).

Tainosho, Y., K. Shibata, and S. Uchiumi, Granitic rocks in Dogo, Oki Islands, Shimane prefecture, Japan, *J. Geol. Soc. Japan*, **97**, 53–60, 1991 (in Japanese with English abstract).

Tamaki, T., K. Suyehiro, J. Allan, J. C. Ingle, Jr., and A. Kenneth, Pisciotto, Tectonic systhesis and implications of Japan Sea ODP drilling, in *Proc. ODP, Sci. Results, 127/128*, edited by K. Tamaki, K. Suyehiro, J. Allan, M. McWilliams, *et al.*, pp. 1333–1350, Ocean Drilling Program, College Station, TX, 1992.

Yamasaki, H., Ceozoic stratigraphy on the north of Sigo Bay, southern part of Oki-Dogo Island, Southwest Japan, *J. Geol. Soc. Japan*, **97**, 917–930, 1991 (in Japanese with English abstract).

Yamasaki, H., The Dogo Group in the Oki Dogo Island, Southwest Japan and the South Oki Ridge, *Mem. Geol. Soc. Japan*, **37**, 277–293, 1992 (in Japanese with English abstract).

Yamasaki, H. and Y. Ganzawa, Fission track ages of the Tertiary Kori and Yui Formations in Dogo, Oki Islands, west Japan, *J. Geol. Soc. Japan*, **95**, 619–622, 1989 (in Japanese).

Yamasaki, H., M. Shitasue, and K. Takayasu, Re-examination of stratigraphic relationship between the Miocene Kori and Kumi Formations in Dogo, Oki Islands, West Japan, *Earth Science*, **45**, 177–190, 1990 (in Japanese with English abstract).

Yamauchi, S. and A. Yoshitani, Tectonic movement in the progressive stage of the Green-Tuff basins—Taking the case of the Miocene series in the eastern part of Shimane Prefecture, western Japan—, *J. Geol. Soc. Japan*, **87**, 711–724, 1981 (in Japanese with English abstract).

Yokota, M., Diatomaceous earth in Dogo, Oki Islands, *Geol. Rept. Shimane Univ.*, **3**, 139–144, 1984 (in Japanese with English abstract).

Yoshitani, A., T. Danhara, and H. Murakami, On the fission track age of Kori Formation belonging to Dogo Group distributed in Dogo Islands, *J. Fac. Edu. Tottori Univ. Natural Science*, **44**, 91–101, 1995 (in Japanese with English abstract).

T. Kojima (e-mail: nd7403@mcs.ipe.ibaraki.ac.jp), M. Okada, H. Ohira, K. Tokieda, H. Komuro, and K. Amano